Why glass elasticity affects the thermodynamics and fragility of super-cooled liquids

Le Yan, Gustavo Düring, and Matthieu Wyart *

*Center for Soft Matter Research, Department of Physics, New York University, New York, NY 10002, USA

Super-cooled liquids are characterized by their fragility: the slowing down of the dynamics under cooling is more sudden and the jump of specific heat at the glass transition is generally larger in fragile liquids than in strong ones. Despite the importance of this quantity in classifying liquids, explaining what aspects of the microscopic structure controls fragility remains a challenge. Surprisingly, experiments indicate that the linear elasticity of the glass – a purely local property of the free energy landscape – is a good predictor of fragility. In particular, materials presenting a large excess of soft elastic modes, the so-called boson peak, are strong. This is also the case for network liquids near the rigidity percolation, known to affect elasticity. Here we introduce a model of the glass transition based on the assumption that particles can organize locally into distinct configurations, which are coupled spatially via elasticity. The model captures the mentioned observations connecting elasticity and fragility. We find that materials presenting an abundance of soft elastic modes have little elastic frustration: energy is insensitive to most directions in phase space, leading to a small jump of specific heat. In this framework strong liquids turn out to lie the closest to a critical point associated with a rigidity or jamming transition, and their thermodynamic properties are related to the problem of number partitioning and to Hopfield nets in the limit of small memory.

Glass transition | Elasticity | Fragility | Rigidity percolation | Boson peak

Introduction

When a liquid is cooled rapidly to avoid crystallization, its viscosity increases up to the glass transition where the material becomes solid. Although this phenomenon was already used in ancient times to mold artifacts, the nature of the glass transition and the microscopic cause for the slowing down of the dynamics remain controversial. Glass-forming liquids are characterized by their fragility [1, 2]: the least fragile liquids are called strong, and their characteristic time scale τ follows approximatively an Arrhenius law $\tau(T) \sim \exp(E_a/k_BT)$, where the activation energy E_a is independent of temperature. Instead in fragile liquids the activation energy grows as the temperature decreases, leading to a sudden slowing-down of the dynamics. The fragility of liquids strongly correlates with their thermodynamic properties [3, 4]: the jump in the specific heat that characterizes the glass transition is large in fragile liquids and moderate in strong ones. Various theoretical works [5–8], starting with Adam and Gibbs, have proposed explanations for such correlations. By contrast few propositions, see e.g. [9–11], have been made to understand which aspects of the microscopic structure of a liquid determines its fragility and the amplitude of the jump in the specific heat at the transition.

Observations indicate that the linear elasticity of the glass is a key factor determining fragility – a fact a priori surprising since linear elasticity is a local property of the energy landscape, whereas fragility is a non-local property characterizing transition between meta-stables states. In particular (i) glasses are known to present an excess of soft elastic modes with respect to Debye vibrations at low frequencies, the so-called boson peak that appears in scattering measurements [12]. The amplitude of the boson peak is strongly anti-correlated with fragility, both in network and molecular liquids: structures presenting an abundance of soft elastic modes tend to be strong [13, 14]. (ii) In network glasses, where particles interact via covalent bonds and via the much weaker Van der Waals interactions, the microscopic structure and the elasticity can be monitored by changing continuously the composition of compounds [15–17]. As the average valence r is increased toward some threshold r_c, the covalent networks display a rigidity transition [18, 19] where the number of covalent bonds is just sufficient to guarantee mechanical stability. Rigidity percolation has striking effects on the thermal properties of super-cooled liquids: in its vicinity, liquids are strong [20] and the jump of specific heat is small [15]; whereas they become fragile with a large jump in specific heat *both* when the valence is increased, and decreased [15, 20]. It was argued [9] that fragility should decrease with valence, at least when the valence is small. There is no explanation however why increasing the valence affects the glass transition properties in a non-monotonic way, and why such properties are extremal when the covalent network acquires rigidity [21].

Recently it has been shown that the presence of soft modes in various amorphous materials, including granular media [22–25], Lennard-Jones glasses [23, 26], colloidal suspensions [27–29] and silica glass [23, 30] was controlled by the proximity of a jamming transition [31], a sort of rigidity transition that occurs for example when purely repulsive particles are decompressed toward vanishing pressure [24]. Near the jamming transition spatial fluctuations play a limited role and simple theoretical arguments [22, 23] capture the connection between elasticity and structure. They imply that soft modes must be abundant near the transition, suggesting a link between observations (i) and (ii). However these results apply to linear elasticity and cannot explain intrinsically non-linear phenomena such as those governing fragility or the jump of specific heat. In this article we propose to bridge that gap by introducing a model for the structural relaxation in super-cooled liquids. Our starting assumption is that particles can organize locally into distinct configurations, which are coupled at different points in space via elasticity. We study what is perhaps the simplest model realizing this idea, and show numerically that it captures qualitatively the relationships between elasticity, rigidity, thermodynamics and fragility. The thermodynamic properties of this model can be treated theoretically within a good accuracy in the temperature range we explore. Our key result is the following physical picture: when
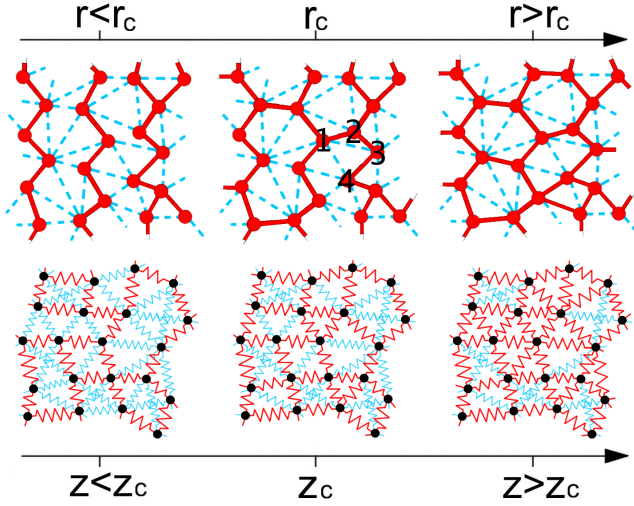
Reserved for Publication Footnotes

Fig. 1. Top row: sketches of covalent networks with different mean valence r around the valence r_c: red solid lines represent covalent bonds; cyan dash lines represent van der Waals interactions. Bottom: sketch of our elastic network model with varying coordination number z (defined as the average number of strong springs in red) around Maxwell threshold z_c; cyan springs have a much weaker stiffness, and model weak interactions.

there is an abundance of soft elastic modes, elastic frustration vanishes, in the sense that a limited number of directions in phase space cost energy. Only those directions contribute to the specific heat, which is thus small. Away from the critical point, elastic frustration increases: more degrees of freedom contribute to the jump of specific heat, which increases while the boson peak is reduced.

Model

Our main assumption is that in a super-cooled liquid, nearby particles can organize themselves into a few distinct configurations. Consider for example covalent networks sketched in Fig. 1, where we use the label $\langle ij \rangle$ to indicate the existence of a covalent bond between particles i and j. If two covalent bonds $\langle 12 \rangle$ and $\langle 34 \rangle$ are adjacent, there exists locally another configuration for which these bonds are broken, and where the bonds $\langle 13 \rangle$ and $\langle 24 \rangle$ are formed instead. These two configurations do not have the same energy in general. Moreover going from one configuration to the other generates a local strain, which creates an elastic stress that propagates in space. In turn, this stress changes the energy difference between local configurations elsewhere in the system. This process leads to an effective interaction between local configurations at different locations.

Our contention is that even a simple description of the local configurations – in our case we will consider two-level systems, and we will make the approximation that the elastic properties do not depend on the levels – can capture several unexplained aspects of super-cooled liquids, as long as the salient features of the elasticity of amorphous materials are taken into account. To incorporate in particular the presence of soft modes in the vibrational spectrum we consider random elastic networks. The elasticity of three types of networks have been studied extensively: networks of springs randomly deposited on a lattice [32], on-lattice self-organized networks [33] and off-lattice random networks with small spatial fluctuations of coordination [34–36]. We shall consider the last class of networks, which are known to capture correctly

the scaling properties of elasticity near jamming, and can be treated analytically [22, 35, 37]. It is straightforward to extend our model to self-organized networks [1]. In our model two kinds of springs connect the N nodes of the network: strong ones, of stiffness k and coordination z, and weak ones, of stiffness k_w and coordination z_w. These networks undergo a rigidity transition as z crosses $z_c = 2d$, where d is the spatial dimension. For $z < z_c$ elastic stability is guaranteed by the presence of the weak springs. As indicated in Fig. 1, this situation is similar to covalent networks, where the weak Van der Waals interactions are required to insure stability when the valence r is smaller than its critical value r_c.

Initially when our network is built, every spring $\langle ij \rangle$ is at rest: the rest length follows $l^0_{\langle ij \rangle} = ||\mathbf{R}^0_i - \mathbf{R}^0_j||$, where $\mathbf{R}^0_i$ is the initial position of the node i. To allow for local changes of configurations we shall consider that any strong spring $\langle ij \rangle$ can switch between two rest lengths: $l_{\langle ij \rangle} = l^0_{\langle ij \rangle} + \epsilon\sigma_{\langle ij \rangle}$, where $\sigma_{\langle ij \rangle} = \pm 1$ is a spin variable. There are thus two types of variables: the $N_s \equiv zN/2$ spin variables $\{\sigma_{\langle ij \rangle}\}$, which we shall denote using the ket notation $|\sigma\rangle$, and the Nd coordinates of the particles denoted by $|\mathbf{R}\rangle$. The elastic energy $\mathcal{E}(|\mathbf{R}\rangle, |\sigma\rangle)$ is a function of both types of variables. The inherent structure energy $\tilde{\mathcal{H}}(|\sigma\rangle)$ associated with any configuration $|\sigma\rangle$ is defined as:

$$\tilde{\mathcal{H}}(|\sigma\rangle) \equiv \min_{|\mathbf{R}\rangle} \mathcal{E}(|\mathbf{R}\rangle, |\sigma\rangle) \equiv k\epsilon^2 \mathcal{H}(|\sigma\rangle) \qquad \textbf{[1]}$$

where we have introduced the dimensionless Hamiltonian $\mathcal{H}$. We shall consider the limit of small ϵ, where the vibrational energy is simply that of harmonic oscillators. In this limit all the relevant information is contained in the inherent structures energy, since including the vibrational energy would increase the specific heat by a constant, which does not contribute to the jump of that quantity at the glass transition. In this limit, linear elasticity implies the form:

$$\mathcal{H}(|\sigma\rangle) = \frac{1}{2}\sum_{\gamma,\beta}\mathcal{G}_{\gamma,\beta}\sigma_\gamma\sigma_\beta + o(\epsilon^2) \equiv \frac{1}{2}\langle\sigma|\mathcal{G}|\sigma\rangle + o(\epsilon^2) \quad \textbf{[2]}$$

where γ and β label strong springs, $\mathcal{G}_{\gamma,\beta}$ is the Green function describing how a dipole of force applied on the contact γ changes the amplitude of the force in the contact β. Note that models where some kind of defects interact elastically, leading to Hamiltonians similar in spirit to that of Eq.(2), have been proposed to investigate the low-temperature properties of glasses [38] and super-cooled liquids [10]. These models however assume continuum elasticity, unlike our model which can incorporate the effects of a rigidity transition and the presence of a boson peak.

$\mathcal{G}_{\gamma,\beta}$ is computed in Supplementary Information (SI) part A and reads:

$$\mathcal{G} = \mathcal{I} - \mathcal{S}_\text{s}\mathcal{M}^{-1}\mathcal{S}_\text{s}^t \qquad \textbf{[3]}$$

where $\mathcal{I}$ is the identity matrix, and $\mathcal{S}_\text{s}$ and the dimensionless stiffness matrix $\mathcal{M}$ are standard linear operators connecting forces and displacements in elastic networks [39]. They can be formally written as:

$$\mathcal{M} = \mathcal{S}_\text{s}^t\mathcal{S}_\text{s} + \frac{k_\text{w}}{k}\mathcal{S}_\text{w}^t\mathcal{S}_\text{w}, \qquad \textbf{[4]}$$

$$\mathcal{S}_\bullet = \sum_{\langle ij \rangle_\bullet \equiv \gamma} |\gamma\rangle\mathbf{n}_{ij}(\langle i| - \langle j|)$$

where $\langle i|\mathbf{R}\rangle \equiv \mathbf{R}_i$, $\langle ij \rangle_\bullet$ indicate a summation over the strong springs ($\bullet = \text{s}$) or the weak springs ($\bullet = \text{w}$). $\mathcal{S}_\bullet$ is a $N_\bullet \times dN$

---

[1]If the network is assumed to present a rigidity window for which a subpart of the system is critical, we expect that within this window thermodynamics and fragility would behave as the critical point $z = z_c$ in the present model.

matrix which projects any displacement field onto the contact space of strong or weak springs. The components of this linear operator are uniquely determined by the unit vectors $\mathbf{n}_{ij}$ directed along the contacts $\langle ij \rangle$ and point toward the node i.

Finally note that the topology of the elastic network is frozen in our model. This addition of frozen disorder is obviously an approximation, as the topology itself should evolve as local configurations change. Our model thus misses the evolution of elasticity with temperature, that presumably affects the slowing down of the dynamics [8] and gives a vibrational contribution to the jump of specific heat [8, 40]. Building models which incorporate this possibility, while still tractable numerically and theoretically, remains a challenge.
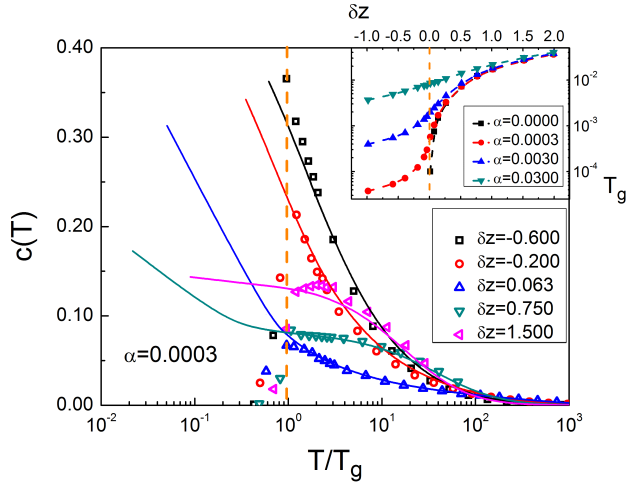

Fig. 2. Specific heat $c(T)$ *v.s.* rescaled temperature T/T_g for various excess coordination $\delta z \equiv z - z_c$ as indicated in legend, for $\alpha = 3 \times 10^{-4}$ and $d = 2$. $c(T)$ displays a jump at the glass transition. Solid lines are theoretical predictions, deprived of any fitting parameters, of our mean-field approximation. They terminate at the Kautzman temperature T_K. Inset: glass transition temperature T_g *vs* δz for several amplitude of weak interactions α, as indicated in legend.
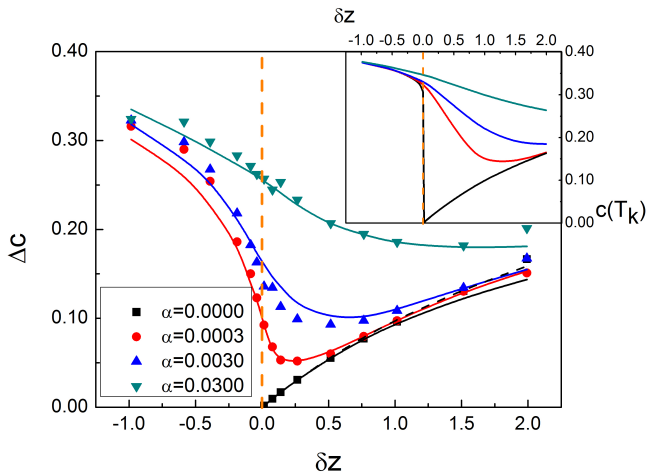

Fig. 3. Jump of specific heat Δc versus excess coordination δz in $d = 2$ for different strength of weak springs α, as indicated in legend. Solid lines are mean-field predictions not enforcing the orthogonality of the $|\delta r_p\rangle$, dashed-line corresponds to the ROM where orthogonality is enforced. In both cases the specific heat is computed at the numerically obtained temperature T_g. Inset: theoretical predictions for Δc *vs* δz computed at the theoretical temperature T_K.

Simulation

Network structure. Random networks with weak spatial fluctuations of coordination can be generated from random packings of compressed soft particles [34–36]. We consider packings with periodic boundary conditions. The centers of the particles correspond to the nodes of the network, of unit mass $m = 1$, and un-stretched springs of stiffness $k = 1$ are put between particles in contact. Then springs are removed, preferably where the local coordination is high, so as to achieve the desired coordination z. In a second phase, $N_{\rm w}$ weak springs are added between the closest unconnected pairs of nodes. The relative effect of those weak springs is best characterized by $\alpha \equiv (z_{\rm w}/d)(k_{\rm w}/k)$, which we modulate by fixing $z_{\rm w} = 6$ and changing $(k_{\rm w}/k)$. Note that an order of magnitude estimate of α in covalent glasses can be obtained by comparing the behavior of the shear modulus G in the elastic networks [34] and in network glasses near the rigidity transition. As shown In Fig. 6 of SI part B, this comparison yields the estimate that $\alpha \in [0.01, 0.05]$.

Thermodynamics. We introduce the rescaled temperature $T = \tilde{T}k_B/(k\epsilon^2)$ where $\tilde{T}$ is the temperature. To equilibrate the system, we perform a one spin-flip Monte Carlo algorithm. The energy $\mathcal{H}$ of configurations are computed using Eq.(2). We use 5 networks of $N = 256$ nodes in two dimensions and $N = 216$ in three dimensions, each run with 10 different initial configurations. Thus our results are averaged on these 50 realizations. We perform 10^9 Monte Carlo steps at each T. The time-average inherent structure energy $E = \langle \mathcal{H} \rangle$ is calculated as a function of temperature, together with the specific heat $C_v = \partial E/\partial T$. The intensive quantity $c(T) \equiv C_v/N_s$ is represented in Fig. 2 for various excess coordination $\delta z = z - z_c$ and $\alpha = 3 \times 10^{-4}$. We observe that the specific heat increases under cooling, until the glass transition temperature T_g where $c(T)$ rapidly vanishes, indicating that the system falls out of equilibrium.

The amplitude of $c(T)$ just above T_g thus corresponds to the jump of specific heat Δc [2], and is shown in Fig. 3. Our key finding is that as the coordination increases, $\Delta c(z)$ varies non-monotonically and is minimal in the vicinity of the rigidity transition for all values of α investigated, as observed experimentally [15]. This behavior appears to result from a sharp asymmetric transition at $\alpha \rightarrow 0$. For $z > z_c$ we observe that $\Delta c(z) \propto \delta z$. The jump in specific heat thus vanishes as $\delta z \rightarrow 0^+$ where the system can be called "perfectly strong". For $z < z_c$, Δc is very rapidly of order one. When α increases, this sharp transition becomes a cross-over, marked by a minimum of $\Delta c(z)$ at some coordination larger but close to z_c.

Dynamics. To characterize the dynamics we compute the correlation function $C(t) = \frac{1}{N_s}\langle \sigma(t)|\sigma(0)\rangle$, which decays to zero at long time in the liquid phase. We define the relaxation time τ as $C(\tau) = 1/2$, and the glass transition temperature T_g as $\tau(T_g)/\tau(\infty) = 10^5$. Finite size effects on τ appear to be weak, as shown in SI part C. The Angell plot representing the dependence of τ with inverse rescaled temperature is shown in the inset of Fig. 4. It is found that the dynamics

---

[2] In our approach the absolute value of the specific heat will depend on the minimal number of particles needed to generate distinct local configurations, and on the number of configurations such a group can generate. If those two numbers are of order one, our model predicts that Δc is of order one per particle or "beads", as observed near the glass transition [6].

[3] When $\alpha \rightarrow 0$ and $\delta z > 0$, $\omega_{BP} \sim \delta z$ and $D(\omega_{BP}) \sim 1$ [22], whereas $G \sim \delta z$ [23], leading to $1/A_{BP} \sim \sqrt{\delta z}$. For $\delta z < 0$, $G \sim -\alpha/\delta z$ [34]. On the other hand the boson peak is governed by the fraction $\sim \delta z$ of floppy modes, which gain a finite frequency $\sim \sqrt{\alpha}$ [35] thus we expect $D(\omega_{BP}) \sim -\delta z/\sqrt{\alpha}$ and $1/A_{BP} \sim \sqrt{-\delta z}$.

follows an Arrhenius behavior for $\alpha \to 0$ and $z \approx z_c$. Away from the rigidity transition, the slowing down of the dynamics is faster than Arrhenius. To quantify this effect we compute the fragility $m \equiv \frac{\partial \log_{10} \tau}{\partial (T_g/T)}|_{T=T_g}$, whose variation with coordination is presented in Fig. 4. Our key finding is that for all weak interaction amplitudes α studied, the fragility depends non-monotonically on coordination and is minimal near the rigidity transition, again as observed empirically [20] in covalent liquids. As was the case for the thermodynamic properties, the fragility appears to be controlled by a critical point present at $\alpha = 0$ and $z = z_c$ where the liquid is strong, and the dynamics is simply Arrhenius. As the coordination changes and $|\delta z|$ increases, the liquid becomes more fragile. The rapid change of fragility near the rigidity transition is smoothed over when the amplitude of the weak interaction α is increased.

Correlating boson peak and fragility. The presence of soft elastic modes in glasses can be analyzed by considering the maximum of $Z(\omega) \equiv \frac{D(\omega)}{D_D(\omega)}$ [12], where $D(\omega)$ is the vibrational density of states and $D_D(\omega) \propto \omega^2$ the Debye model for this quantity. The maximum of $Z(\omega)$, $A_{BP} = Z(\omega_{BP})$ defines the boson peak frequency ω_{BP} [12] and it normalized amplitude A_{BP} [13]. The inverse of A_{BP} was shown to strongly correlate with fragility [13, 14] both in molecular liquids and covalent networks.

To test if our model can capture this behavior we compute the density of states via a direct diagonalization of the stiffness matrix, see Eq.(4). To compute $Z(\omega)$ the Debye density of states is estimated as $D(\omega) \sim \omega^2/G^{3/2}$ where G is the shear modulus (bulk and shear moduli scale identically in this model, see e.g. [37]). Then we extract the maximum $A_{BP} = Z(\omega_{BP})$. The dependence of $1/A_{BP}$ is represented in Fig. 5 and shows a minimum near the rigidity transition, and even a cusp in the limit $\alpha \to 0$. This behavior can be explained in terms of previous theoretical results on the density of states near the rigidity transition, that supports that $1/A_{BP} \sim |\delta z|^{1/2}$ when $\alpha \to 0$ [3].

Fig. 5 shows that $1/A_{BP}$ and the liquid fragility m are correlated in our model, thus capturing observations in molecular liquids. The model also predicts that $1/A_{BP}$ and the jump of specific heat are correlated. Note that the correlation between fragility and A_{BP} is not perfect, and that two branches, for glasses with low and with high coordinations, are clearly distinguishable. In general we expect physical properties to depend on the full structure of the density of states, as will be made clear for the thermodynamics of our model below. The variable A_{BP}, which is a single number, cannot capture fully this relationship. In our framework it is a useful quantity however, as it characterizes well the proximity of the jamming transition.

Theory

Thermodynamics in the absence of weak interactions ($\alpha = 0$). In the absence of weak springs the thermodynamics is non-trivial if $z \geq z_c$, otherwise the inherent structure energies are all zero. Then Eq.(4) implies $\mathcal{M} = \mathcal{S}_s^t \mathcal{S}_s$, and Eq.(3) leads to $\mathcal{G} = \mathcal{I} - \mathcal{S}_s (\mathcal{S}_s^t \mathcal{S}_s)^{-1} \mathcal{S}_s^t$. Inspection of this expression indicates that $\mathcal{G}$ is a projector on the kernel of $\mathcal{S}_s^t$, which is generically of dimension $N_s - Nd \equiv \delta z N/2$. This kernel corresponds to all the sets of contact forces that balance forces on each node [23]. We denote by $|\delta r_p\rangle, p = 1, ..., \delta z N/2$ an orthonormal basis of this space. We may then rewrite $\mathcal{G} = \sum_p |\delta r_p\rangle\langle\delta r_p|$ and Eq.(2)

as:

$$\mathcal{H}(|\sigma\rangle) = \frac{1}{2} \sum_{p=1}^{\delta z N/2} \langle\sigma|\delta r_p\rangle^2 \qquad [5]$$

Eq.(5) is a key result, as it implies that near the rigidity transition the number $\delta z N/2$ of directions of phase space that cost energy vanishes. Only those directions can contribute to the specific heat, which must thus vanish linearly in δz as the rigidity transition is approached from above.

Eq.(5) also makes a connection between strong liquids in our framework and well-know problems in statistical mechanics. In particular Eq.(5) is similar to that describing Hopfield nets [41] used to store $\delta z N/2$ memories consisting of the spin states $|\delta r_p\rangle$. The key difference is the sign: in Hopfield nets memories correspond to meta-stables states, whereas in our model the vectors $|\delta r_p\rangle$ corresponds to maxima of the energy. A particularly interesting case is $\delta z N/2 = 1$, the closest point to the jamming transition which is non-trivial. In this situation the sum in Eq.(5) contains only one term: $\mathcal{H}(|\sigma\rangle) = \frac{1}{2}\langle\sigma|\delta r_1\rangle^2 = \frac{1}{2}(\sum_{\alpha=1}^{N_s} \delta r_{1,\alpha}\sigma_\alpha)^2$. This Hamiltonian corresponds to the NP complete partitioning problem [42], where given a list of numbers (the $\delta r_{1,\alpha}$) one must partition this list into two groups whose sums are as identical as pos-
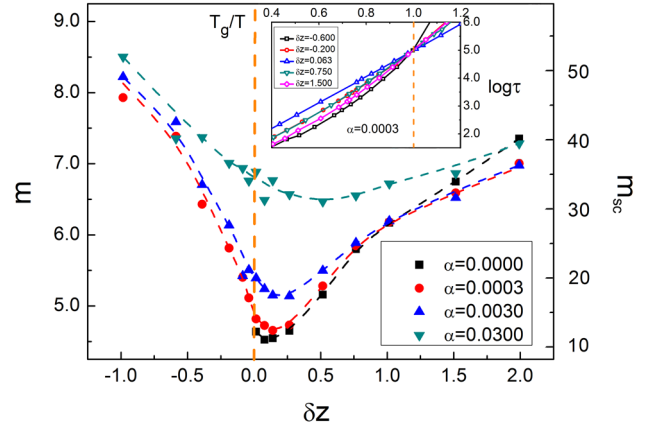

Fig. 4. Fragility m and rescaled fragility m_{sc} extrapolated to the experimental dynamical range (see SI part D for a definition) versus excess coordination δz for different strength of weak interactions α as indicated in legend, in $d = 2$. Dash dot lines are guide to the eyes, and reveal the non-monotonic behavior of m near the rigidity transition. Inset: Angell plot representing $\log \tau$ $v.s.$ inverse temperature T_g/T for different δz and $\alpha = 3 \times 10^{-4}$.
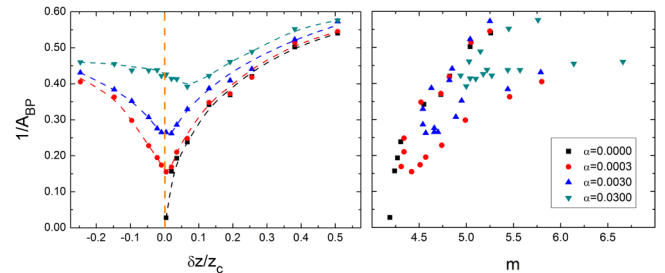

Fig. 5. Left: Inverse boson peak amplitude $1/A_{BP}$ versus excess coordination δz in our $d = 3$ elastic network model, for different weak interaction strenghts as indicated in legend. Dash dot lines are drawn to guide one's eyes. Right: Inverse boson peak amplitude $1/A_{BP}$ versus fragility m for different weak springs α.

sible. Thermodynamically this problem is known [43] to map into the random energy model [44] where energy levels are randomly distributed.

It is in general very difficult to compute the thermodynamic functions of the problem defined by Eq.(5) because the vectors $|\delta r_p\rangle$ present spatial correlations, as must be the case since the amplitude of the interaction kernel $\mathcal{G}_{\gamma,\beta}$ must decay with distance. However this effect is expected to be mild near the rigidity transition. Indeed there exists a diverging length scale at the transition, see [35] for a recent discussion, below which $\mathcal{G}_{\gamma,\beta}$ is dominated by fluctuations and decays mildly with distance. Beyond this length scale $\mathcal{G}_{\gamma,\beta}$ presents a dipolar structure, as in a standard continuous elastic medium. We shall thus assume that $|\delta r_p\rangle$ are random unitary vectors, an approximation of mean-field character expected to be good near the rigidity transition.

Within this approximation, the thermodynamic properties can be derived for any spectrum of $\mathcal{G}$ [45]. If the orthogonality of the vectors $|\delta r_p\rangle$ is preserved, the Hamiltonian of Eq.(5) corresponds to the Random Orthogonal Model (ROM) whose thermodynamic properties have been derived [45] as well as some aspects of the dynamics [46]. Comparison of the specific heat of our model and the ROM predictions of [45] is shown in Fig. 3 and are found to be very similar. For sake of simplicity, in what follows we shall also relax the orthogonal condition on the vectors $|\delta r_p\rangle$. This approximation allows for a straightforward analytical treatment in the general case $\alpha \neq 0$, and is also very accurate near the rigidity transition since the number of vectors $\delta z N/2$ is significantly smaller than the dimension of the space dN they live in, making random vectors effectively orthogonal. Under these assumptions we recover the random Hopfield model with negative temperature.

In the parameter range of interest, the Hopfield free energy $\mathcal{F} = \overline{\ln(\mathcal{Z})}$ (here $\overline{(...)}$ represents the disorder average on the $|\delta r_p\rangle$) is approximated very precisely by the annealed free energy $\ln(\overline{\mathcal{Z}})$ (this is obviously true for the number partitioning problem that maps to the Random Energy Model), which can be easily calculated. Indeed in our approximations the quantities $X_p \equiv \langle \sigma|\delta r_p\rangle$ are independent gaussian random variables of variance one, and:

$$\overline{\mathcal{Z}} \propto \int \left(\prod_{p=1}^{N\delta z/2} dX_p \frac{1}{\sqrt{2\pi}} e^{-X_p^2/2} \right) e^{-\frac{1}{2T}\sum_p X_p^2} \quad [\textbf{6}]$$

Performing the Gaussian integrals we find:

$$c(T) = \frac{\delta z}{2z} \frac{1}{(1+T)^2} \quad [\textbf{7}]$$

The Kautzman temperature defined as $s(T_K) = 0$ is found to follow $T_K \approx \frac{2}{e} 2^{-2z/\delta z}$. Eq.(7) evaluated at T_g is tested against the numerics in Fig. 3 and performs remarkably well for the range of coordination probed.

General case $(\alpha \neq 0)$. To solve our model analytically in the presence of weak interactions, we make the additional approximation that the associated coordination $z_\mathrm{w} \to \infty$, while keeping $\alpha \equiv z_\mathrm{w} k_\mathrm{w}/(kd)$ constant. In this limit weak springs lead to an effective interaction between each node and the center of mass of the system, that is motionless. Thus the restoring force stemming from weak interactions $|\mathbf{F}_\mathrm{w}\rangle$ follows $|\mathbf{F}_\mathrm{w}\rangle = -\alpha|\delta\mathbf{R}\rangle$, leading to a simple expression in the stiffness matrix Eq.(4) for the weak spring contribution $\frac{k_\mathrm{w}}{k} \mathcal{S}_\mathrm{w}^t \mathcal{S}_\mathrm{w} = \alpha\mathcal{I}$. It is useful to perform the eigenvalue decomposition:

$$\mathcal{S}_\mathrm{s}^t \mathcal{S}_\mathrm{s} = \sum_\omega \omega^2 |\delta\mathbf{R}_\omega\rangle\langle\delta\mathbf{R}_\omega| \quad [\textbf{8}]$$

where $|\delta\mathbf{R}_\omega\rangle$ is the vibrational mode of frequency ω in the elastic network without weak interactions. We introduce the orthonormal eigenvectors in contact space $|\delta r_\omega\rangle \equiv \mathcal{S}_\mathrm{s}|\delta\mathbf{R}_\omega\rangle/\omega$ defined for $\omega > 0$. For $\delta z < 0$ these vectors form a complete basis of that space, of dimension N_s. When $\delta z > 0$ however, this set is of dimension $Nd < N_s$, and it must be completed by the kernel of $\mathcal{S}_\mathrm{s}^t$, i.e. the set of the $|\delta r_p\rangle, p = 1, ..., \delta z N/2$ previously introduced. Using this decomposition in Eq.(3,4) we find:

$$\mathcal{H}(|\sigma\rangle) = \frac{1}{2} \sum_{p=1}^{\delta z N/2} \langle\sigma|\delta r_p\rangle^2 + \frac{1}{2} \sum_{\omega>0} \frac{\alpha}{\alpha+\omega^2} \langle\sigma|\delta r_\omega\rangle^2 \quad [\textbf{9}]$$

where the first term exists only for $\delta z > 0$. Using the mean field approximation that the set of $|\delta r_p\rangle$ and $|\delta r_\omega\rangle$ are random gaussian vectors, the annealed free energy is readily computed, as shown in SI part E. We find in particular for the specific heat:

$$c(T) = \frac{\delta z}{2z} \frac{\theta(\delta z)}{(1+T)^2} + \frac{1}{2N_s} \sum_{\omega>0} \left(\frac{\alpha}{\alpha+(\omega^2+\alpha)T} \right)^2 \quad [\textbf{10}]$$

where $\theta(x)$ is the unitary step function. To compare this prediction with our numerics without fitting parameters, we compute numerically the vibrational frequencies for each value of the coordination. Our results are again in excellent agreement with our observations, as appears in Figs. 5, 5.

To obtain the asymptotic behavior near jamming, we replace the summation over frequencies in Eq.(10) by an integral $\sum_{\omega>0} \to N_s \int d\omega D(\omega)$. The associated density of vibrational modes $D(\omega)$ in such networks has been computed theoretically [22, 35, 37]. These results allows us to compute the scaling behavior of thermodynamic properties near the rigidity transition, see SI part F. We find that the specific heat increases monotonically with decreasing temperature. Its value at the Kautzman temperature thus yields an upperbound on the jump of specific heat. In the limit $\alpha \to 0$, we find that a sudden discontinuity of the jump of specific heat occurs at the rigidity transition:

$$c(T_K) \quad \sim \quad \frac{\delta z}{2z} \qquad \text{for } \delta z > 0 \qquad [\textbf{11}]$$

$$\lim_{\delta z \to 0^-} c(T_K) \quad \sim \quad \frac{\pi z_c}{8z} \qquad [\textbf{12}]$$

Eq.(11) states that adding weak interactions is not a singular perturbation for $\delta z > 0$, and we recover Eq.(7). On the other hand for $\delta z < 0$, the energy of inherent structures is zero in the absence of weak springs, which thus have a singular effect. The relevant scale of temperature is then a function of α. In particular we find that the Kautzman temperature is sufficiently low that all the terms in the second sum of Eq.(10) contribute significantly to the specific heat, which is therefore large as Eq.(12) implies. Thus as the coordination decreases below the rigidity transition, one goes discontinuously from a regime where at the relevant temperature scale the energy landscape consists of a vanishing number of costly directions in phase space, whose cost is governed by the strong interaction k, to a regime where the weak interaction α is the relevant one, and where at the relevant temperature scale all directions in phase space contribute to the specific heat.

Note that although the sharp change of thermodynamic behavior that occurs at the rigidity transition is important conceptually, empirically a smooth cross-over will always be observed. This is the case because (i) α is small but finite. As α increases this sharp discontinuity is replaced by a cross-over at a coordination $\delta z \sim \ln(1/\alpha)^{-1}$ (see SI part F) where $c(T_K, z)$ is minimal, as indicated in the inset of Fig. 3. (ii)

The Kautzman temperature range is not accessible dynamically, i.e. $T_g >> T_K$ near the rigidity transition. Comparing Fig. 3 with its inset, our theory predicts that the minimum of $c(T_g)$ is closer to z_c and more pronounced than at T_K.

Discussion

Previous work [31] has shown that well-coordinated glasses must have a small boson peak, which increases as the coordination (or valence for network glasses) is decreased toward the jamming (or rigidity) transition. Here we have argued that as this process occurs, elastic frustration vanishes: thanks to the abundance of soft modes, any configuration (conceived here as a set of local arrangements of the particles) can relax more and more of its energy as jamming is approached from above. As a result, the effective number of degrees of freedom that cost energy and contribute to the jump of specific heat at the glass transition vanishes. As the coordination is decreased further below the rigidity transition, the scale of energy becomes governed by the weak interactions (such as Van der Waals) responsible for the finite elasticity of the glass. At that scale, all direction in phase space have a significant cost and the specific heat increases. This view potentially explains why linear elasticity strongly correlates to key aspects of the energy landscape in network and molecular glasses [13–16]. This connection we propose between structure and dynamics can also be tested numerically. Our results are consistent with the observation that soft particles become more fragile when compressed away from the random close packing [47] [4]. Another interesting parameter to manipulate is the amplitude of weak interactions, which can be increased by adding long-range forces to the interaction potential [23,26]. According to our analysis, doing so should increase fragility, in agreement with existing observations [48].

The model of the glass transition we introduced turns out to be a spin glass model, with the specificity that (i) the interaction is dipolar in the far field, and that (ii) the sign of the interaction is approximatively random below some length scale l_c that diverges near jamming, where the coupling matrix has a vanishingly small rank. Applying spin glass models to structural glasses have a long history. In particular the Random First Order Transition theory (RFOT) [6] is based on mean-field spin glass models that display a thermodynamic transition at some T_K where the entropy vanishes. A phenomenological description of relaxation in liquids near T_K based on the nucleation of random configurations leads to a diverging time scale and length scale ξ at T_K [6,7]. One limitation of this approach is that no finite dimensional spin models with two-body interactions have been shown to follow this scenario so far [49], and it would thus be important to know if our model does display a critical point at finite temperature. Our model will also allow one to investigate the generally neglected role of the action at a distance allowed by elasticity, characterized by a scale l_c. In super-cooled liquids heterogeneities of elasticity (that correlates to irreversible rearrangements) can be rather extended [50] suggesting that l_c is large. This length scale may thus play an important role in a description of relaxation in liquids, and in deciphering the relationship between elastic and dynamical heterogeneities.

SUPPLEMENTARY INFORMATION

A. Stiffness and Coupling matrices

Consider a network of N nodes connected by N_c springs. If an infinitesimal displacement field $|\delta\mathbf{R}\rangle$ is imposed on the nodes, the change of length of the springs can be written as a vector $|\delta r\rangle$ of dimension N_c. For small displacements this relation is approximately linear: $|\delta r\rangle = \mathcal{S}|\delta\mathbf{R}\rangle$, where $\mathcal{S}$ is an $N_c \times Nd$ matrix. To simplify the notation, we write $\mathcal{S}$ as an $N_c \times N$ matrix of components of dimensions d, which gives $\mathcal{S}_{\gamma,i} \equiv \partial r_\gamma / \partial \mathbf{R}_i = \delta_{\gamma,i}\mathbf{n}_\gamma$, where $\delta_{\gamma,i}$ is non-zero only if the contact γ includes the particle i, and $\mathbf{n}_\gamma$ is the unit vector in the direction of the contact γ, pointing toward the node i. Using the bra-ket notation, we can rewrite $\mathcal{S} = \sum_{\langle ij\rangle \equiv \gamma} |\gamma\rangle \mathbf{n}_\gamma(\langle i| - \langle j|)$, where the sum is over all the springs of the network. Note that the transpose $\mathcal{S}^t$ of $\mathcal{S}$ relates the set of contact forces $|f\rangle$ to the set $|\mathbf{F}\rangle$ of unbalanced forces on the nodes: $|\mathbf{F}\rangle = \mathcal{S}^t|f\rangle$, which simply follows from the fact that $\mathbf{F}_i = \sum_\gamma \delta_{\gamma,i}f_\gamma\mathbf{n}_\gamma = \sum_\gamma f_\gamma\mathcal{S}_{\gamma,i}$ [39].

The stiffness matrix $\tilde{\mathcal{M}}$ is a linear operator connecting external forces to the displacements: $\tilde{\mathcal{M}}|\delta\mathbf{R}\rangle = |\mathbf{F}\rangle$. Introducing the $N_c \times N_c$ diagonal matrix $\mathcal{K}$, whose components are the spring stiffnesses $\mathcal{K}_{\gamma\gamma} = k_\gamma$, we have for harmonic springs $|f\rangle = \mathcal{K}|\delta r\rangle$. Applying $\mathcal{S}^t$ on each side of this equation, we get $|\mathbf{F}\rangle = \mathcal{S}^t|f\rangle = \mathcal{S}^t\mathcal{K}\mathcal{S}|\delta\mathbf{R}\rangle$, which thus implies [39]:

$$\tilde{\mathcal{M}} = \mathcal{S}^t\mathcal{K}\mathcal{S}.$$

Let us assume that starting from a configuration where all springs are at rest, the rest lengths of the springs are changed by some amount $|y\rangle$. This will generate an unbalanced force field $|\mathbf{F}\rangle = \mathcal{S}^t\mathcal{K}|y\rangle$ on the nodes, leading to a displacement $|\delta\mathbf{R}\rangle = \tilde{\mathcal{M}}^{-1}\mathcal{S}^t\mathcal{K}|y\rangle$. The elastic energy $\mathcal{E} = \frac{1}{2}\langle y-\delta r|\mathcal{K}|y-\delta r\rangle$ is minimal for this displacement and the corresponding energy $\tilde{\mathcal{H}}$ is:

$$\tilde{\mathcal{H}}(|y\rangle) = \frac{1}{2}\langle y|\mathcal{K} - \mathcal{K}\mathcal{S}\tilde{\mathcal{M}}^{-1}\mathcal{S}^t\mathcal{K}|y\rangle. \qquad \textbf{[SI-1]}$$
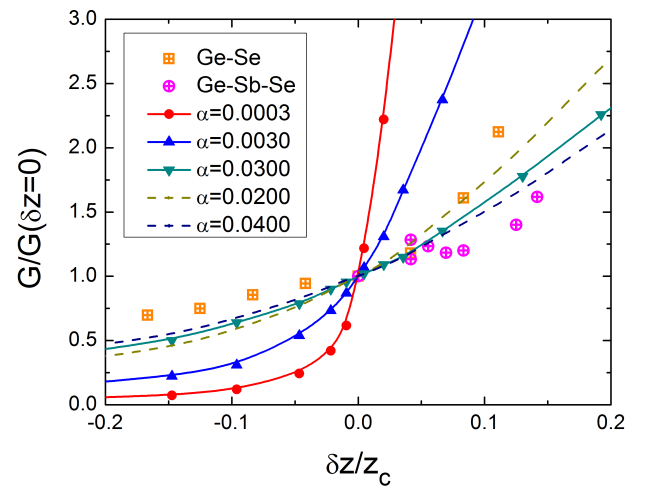

Fig. 6. Squares show the shear modulus G normalized by its value at the rigidity threshold for Ge-Se, taken from Ref. [53]. Circles show G for Ge-Sb-Se, taken from Ref. [54]. Lines display the shear modulus G for network models in $d = 3$ using different α, as indicated in the legend.

---

[4]A quantitative treatment of the vicinity of random close packing would require including the dependence of elasticity on temperature neglected here.

In our model, $y_\gamma = 0$ for weak springs and $y_\gamma = \epsilon\sigma_\gamma$ for strong springs of stiffness k, implying that $\mathcal{K}|y\rangle = k|y\rangle$. Introducing the dimensionless stiffness matrix $\mathcal{M} \equiv \tilde{\mathcal{M}}/k$ and the restriction $\mathcal{S}_s^t$ of the operator $\mathcal{S}^t$ on the subspace of strong contacts of dimension N_s, i.e. $\mathcal{S}_s^t|\sigma\rangle \equiv \mathcal{S}^t|y\rangle$, Eq.(SI-1) yields:

$$\mathcal{H}(|\sigma\rangle) = \frac{1}{2}\langle\sigma|\mathcal{G}|\sigma\rangle \text{ where } \mathcal{G} = \mathcal{I} - \mathcal{S}_s\mathcal{M}^{-1}\mathcal{S}_s^t,$$

where $\mathcal{I}$ is the identity matrix, and $\mathcal{G}$ is the coupling matrix used in the main text. Note that in our model the diagonal matrix $\mathcal{K}$ contains only two types of coefficients k_w and k, corresponding to the stiffnesses of weak springs and stiff springs respectively. Then the dimensionless stiffness matrix can be written as $\mathcal{M} = \mathcal{S}_s^t\mathcal{S}_s + \frac{k_w}{k}\mathcal{S}_w^t\mathcal{S}_w$, where $\mathcal{S}_w^t$ is the projection of the operator $\mathcal{S}^t$ on the subspace of weak contacts.

B. Shear Modulus of the random elastic networks

An explicit expression for the shear modulus G of an elastic network can be found using linear response theory [51,52]. In particular, let us consider the shear on the (x, y) plane. In the contact vector space, a shear strain can be written as $\delta|y^{sh}\rangle$ with $\delta \ll 1$ which represents the amplitude of the strain and $|y^{sh}\rangle$ corresponds to a unit shear strain. The components of $|y^{sh}\rangle$ are given by $y_\gamma^{sh} = \frac{\Delta x_\gamma \Delta y_\gamma}{l_\gamma}$, where l_γ is the rest length of the spring γ, and Δx_γ and Δy_γ are its projections along the x and y directions. From the last section (A), we can obtain the total energy induced by a shear strain $\tilde{\mathcal{H}}(|y^{sh}\rangle)\delta^2$; hence the shear modulus $G = 2\tilde{\mathcal{H}}(|y^{sh}\rangle)/V$.

To estimate the value of α, we consider the dependence of the shear modulus with coordination or valence in the vicinity of the rigidity transition, which is smooth for large α and sudden for small α in our networks, see Fig. 6. Comparing networks and real chalcogenide glasses we find that the cross-over in the elastic modulus is qualitatively reproduced for $\alpha \in [0.01, 0.05]$.

C. Finite size effects on fragility

To estimate the role of finite size effects on the dynamics, we use two different system sizes $N = 64$ and $N = 256$. As shown in Fig. 7, the Angell plot for the relaxation time, and therefore our estimation of the fragility, appears to be nearly independent of the system size. Note, however, that the correlation function $C(t)$ shows some finite size effects very close to the isostatic point ($z = z_c, \alpha = 0$), but that it does not affect our measure of τ significantly. In particular we find that near isostaticity, the distribution of relaxation time is broad for small systems, and becomes less and less so when the system size increases. We noticed that this effect also disappears if a two-spin flips Monte-Carlo is used, instead of the one-spin flip algorithm we perform.

D. Rescale fragility with different dynamical range

The value of fragility depends on the definition of glass transition, in particular on the dynamical range. In super-cooled liquids the glass transition occurs when the relaxation time is about 10^{16} larger than the relaxation time at high temperature. Thus the dynamical range in experiments (which corresponds to the fragility of a perfectly Arrhenius liquid) is $R = 16$. In our simulation, the same quantity is $R = 5$. It is possible however to rescale our values of fragility to compare with experimental data, if we extrapolate the dynamics. We shall assume a Vogel-Fulcher-Tammann (VFT) relation at low
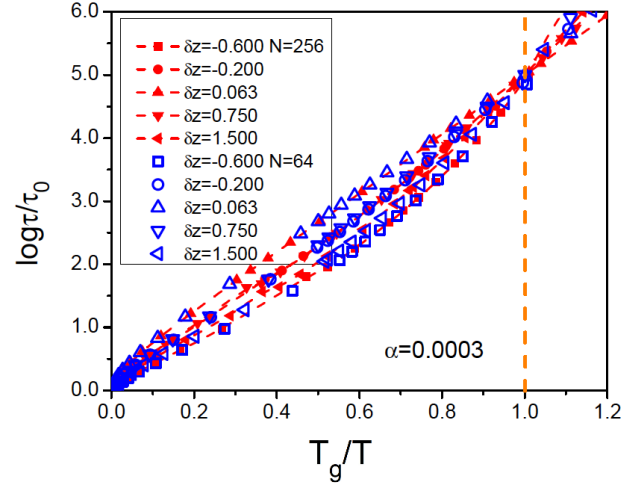

Fig. 7. Angell plot representing $\log\tau$ v.s. inverse temperature T_g/T for different δz and two system sizes $N = 64$ and $N = 256$, $\alpha = 0.0003$.

temperature,

$$\log_{10}\frac{\tau(T)}{\tau_0} = \frac{A}{T - T_0},$$

We define the dynamical range as:

$$R = \log_{10}\frac{\tau(T_g)}{\tau_0} = \frac{A}{T_g - T_0}.$$

Thus we can express the fragility as:

$$m_R = \left.\frac{\partial \log_{10}\tau(T)/\tau_0}{\partial T_g/T}\right|_{T=T_g} = R + R^2\frac{T_0}{A}. \qquad [\text{SI-2}]$$

T_0 and A are assumed to be independent of dynamical range. Using the notation $m = m_5$ and $m_{sc} = m_{16}$ we get from Eq.(SI-2):

$$m_{sc} = 16 + \frac{16^2}{5^2}(m - 5) = 10.24m - 35.2$$

The amplitude of fragility we find turn out to be comparable to experiments when $\alpha = 0.03$, in particular for $z \geq z_c$. For the smallest coordination explored our results underestimate somewhat the fragility, slightly above 50 in our model and about 80 experimentally. This is not surprising considering that our model is phenomenological, and the extrapolation we made to compare different dynamical ranges.

E. Canonical ensemble approach with weak springs

In the case where $\alpha \neq 0$, the annealed free energy can be easily calculated under the assumption that $|\delta r_p\rangle$ and $|\delta r_\omega\rangle$ are random Gaussian vectors. The Hamiltonian in Eq.(10) can be rewritten as:

$$\mathcal{H} = \frac{1}{2}\sum_{p=1\ldots\delta z N/2} X_p^2 + \frac{1}{2}\sum_{\omega>0}\frac{\alpha}{\alpha+\omega^2}X_\omega^2,$$

where $X_p = \langle\delta r_p|\sigma\rangle$ and $X_\omega = \langle\delta r_\omega|\sigma\rangle$ represent independent random variables for each configuration $|\sigma\rangle$. In the thermodynamic limit the random variables X_p and X_ω are Gaussian distributed with zero mean and unit variance. The averaged partition function is given by:

$$\overline{\mathcal{Z}} = 2^{N_s} \int e^{-\mathcal{H}/T} \prod_p \frac{e^{-\frac{X_p^2}{2}}}{\sqrt{2\pi}} dX_p \prod_\omega \frac{e^{-\frac{X_\omega^2}{2}}}{\sqrt{2\pi}} dX_\omega$$

$$= 2^{N_s} \prod_{p=1}^{\delta z N/2} \left(1 + \frac{1}{T}\right)^{-1/2} \prod_{\omega>0} \left(1 + \frac{\alpha/T}{\alpha + \omega^2}\right)^{-1/2}.$$

From the average partition function the density of free energy per spring $f(T)$ and any other thermodynamic quantities are readily computed. In particular, the energy density $\varepsilon(T)$, the specific heat $c(T)$ and the entropy density $s(T)$ write:

$$f(T) = \frac{T}{2N_s} \left[\sum_{p=1}^{\delta z N/2} \ln\left(1 + \frac{1}{T}\right) + \sum_{\omega>0} \ln\left(1 + \frac{\alpha/T}{\alpha + \omega^2}\right) \right] - T \ln 2$$

$$\varepsilon(T) = \frac{1}{2N_s} \left[\sum_{p=1}^{\delta z N/2} \frac{T}{1+T} + \sum_{\omega>0} \frac{\alpha T}{\alpha + (\omega^2 + \alpha)T} \right]$$

$$c(T) = \frac{1}{2N_s} \left[\sum_{p=1}^{\delta z N/2} \frac{1}{(1+T)^2} + \sum_{\omega>0} \left(\frac{\alpha}{\alpha + (\omega^2 + \alpha)T} \right)^2 \right]$$

[SI-2]

$$s(T) = \ln 2 - \frac{1}{2N_s} \sum_{p=1}^{\delta z N/2} \left[\ln(1 + \frac{1}{T}) - \frac{1}{1+T} \right]$$
$$- \frac{1}{2N_s} \sum_{\omega>0} \left[\ln\left(1 + \frac{\alpha/T}{\alpha + \omega^2}\right) - \frac{\alpha}{\alpha + (\omega^2 + \alpha)T} \right].$$

In the limit $\alpha \to 0$, for any finite temperature T, the sum over the vibration modes ($\omega > 0$) vanishes, and we recover the expressions in the absence of weak springs for pure rigid networks. Note that Eq.(SI-2) corresponds to Eq.(11) in the article.

F. Continuous density of states limit: Analytical results

In the thermodynamic limit $N \to \infty$, we can replace the sum over frequencies by an integral: $\sum_{\omega>0} \to N_s \int d\omega D(\omega)$ for $\delta z \leq 0$, and $\sum_{\omega>0} \to Nd \int d\omega D(\omega)$ for $\delta z > 0$. The density of states $D(\omega)$ is the distribution of vibrational modes of random elastic networks, which has been computed theoretically [22,35,37]. There are two frequency scales in the random network : $\omega^* \sim |\delta z|$ above which a plateau of soft modes exist, and a cut-off frequency $\omega_c \sim 1$. Below ω^*, rigid networks show plane wave modes [22,34,37] with a characteristic Debye regime $D(\omega) \sim \omega^2$, unlike floppy networks, which show no modes in this gap [35].

It turns out that the Debye regime contribution to the integrals is negligible near the jamming threshold. To capture the scaling behavior near jamming, we approximate $D(\omega)$ by a square function. This simplified description allows further analytical progress while preserving the same qualitative behavior. Since the Debye regime can be neglected, we choose:

$$D(\omega) = \begin{cases} \frac{1}{\omega_c - \omega^*} & \omega^* \leq \omega \leq \omega_c \quad \delta z \leq 0 \\ \frac{1}{\omega_c} & 0 \leq \omega \leq \omega_c \quad \delta z > 0. \end{cases}$$

Considering $\omega^* = \frac{|\delta z|}{z_c}\omega_c$, the cut-off frequency $\omega_c \sim 1$ is the only fitting parameter of the simplified continuum model. Rescaling as $\alpha \to \alpha\omega_c^2$, we obtain that all the thermodynamic functions depend uniquely on $\alpha = \frac{z_w k_w}{dk\omega_c^2}$, T and δz. In particular, the specific heat is:

$$c(T, \delta z, \alpha) = \begin{cases} \frac{z_c}{4z} \frac{\sqrt{\alpha(1+1/T)}}{(1+T)^2} \left[\arctan(\frac{1}{\sqrt{\alpha(1+1/T)}}) \right. \\ \quad + \frac{\sqrt{\alpha(1+1/T)}}{1+\alpha(1+1/T)} + \arctan(\frac{\delta z/z_c}{\sqrt{\alpha(1+1/T)}}) \\ \quad \left. + \frac{\delta z}{z_c} \frac{\sqrt{\alpha(1+1/T)}}{\delta z^2/z_c^2 + \alpha(1+1/T)} \right] & \delta z \leq 0 \\[2em] \frac{z_c}{4z} \frac{\sqrt{\alpha(1+1/T)}}{(1+T)^2} \left[\arctan(\frac{1}{\sqrt{\alpha(1+1/T)}}) \right. \\ \quad \left. + \frac{\sqrt{\alpha(1+1/T)}}{1+\alpha(1+1/T)} \right] + \frac{\delta z}{2z} \frac{1}{(1+T)^2} & \delta z > 0. \end{cases}$$

We compute the jump of specific heat at the Kautzman temperature, where the entropy vanishes $s(T_K, \delta z, \alpha) = 0$. In the continuous limit, the equations for T_K can be approximated by:

$$\ln 2 \approx \frac{z_c}{2z} \left[\ln(1 + \frac{\alpha}{T_K}) + 2\sqrt{\frac{\alpha}{T_K}} \arctan\sqrt{\frac{T_K}{\alpha}} \right] - \frac{\delta z}{2z}\theta(\delta z)\ln T_K,$$

where the conditions $|\delta z| \ll z_c$ and $\alpha \sim k_w/k \ll 1$ have been used. There is no simple analytical expression for T_K, however, one can observe the existence of two asymptotic regimes: $T_K \sim \alpha$ for $\delta z \ll |1/\ln\alpha|$ and $T_K \sim 2^{-2z/\delta z}$ for $\delta z \gg |1/\ln\alpha|$. Then the specific heat at the transition temperature is given by:

$$c(T_K, \delta z, \alpha) \sim \begin{cases} \frac{z_c}{4z} \frac{\pi}{2} & \delta z \ll |1/\ln\alpha| \\[1em] \frac{\delta z}{2z} & \delta z \gg |1/\ln\alpha|. \end{cases}$$

From these asymptotic behaviors one gets that the specific heat display a non-monotonous behavior with coordination, with a minimum whose position scales as $\delta z \sim |1/\ln\alpha|$.

1. Ediger MD, Angell CA, Nagel SR (1996) Supercooled liquids and glasses. J Phys Chem 100:13200–13212.
2. Debenedetti PG, Stillinger FH (2001) Supercooled liquids and the glass transition. Nature 410:259–267.
3. Wang L, Angell CA, Richert R (2006) Fragility and thermodynamics in nonpolmeric glass forming liquids. J Chem Phys 125:074505.
4. Martinez LM, Angell CA (2001) A thermodynamic connection to the fragility of glass-forming liquids. Nature 410:663–667.
5. Adam A, Gibbs JH (1965) On the temperature dependence of cooperative relaxation properties in glass-forming liquids. J Chem Phys 43:139.
6. Lubchenko V, Wolynes P (2007) Theory of structural glasses and supercooled liquids. Annu Rev Phys Chem 58:235–266.
7. Bouchaud JP, Biroli G (2004) On the Adam-Gibbs-Kirkpatrick-Thirumalai-Wolynes scenario for the viscosity increase in glasses. J Chem Phys 121:7347.
8. Dyre JC (2005) The glass transition and elastic models of glass-forming liquids. Rev Mod Phys 78:953–972.
9. Hall RW, Wolynes PG (2003) Microscopic theory of network glasses. Phys Rev Lett 90:085505.
10. Bevzenko D Lubchenko V (2009) Stress distribution and the fragility of supercooled melts. J Phys Chem B 113:16337.
11. Shintani H, Tanaka H (2008) Universal link between the boson peak and transverse phonons in glass. Nature Material 7:870–877.
12. Anderson AC (1981) in Amorphous Solids, Low Temperature Properties, ed Phillips WA (Springer, Berlin).
13. Novikov VN, Ding Y, Sokolov AP (2005) Correlation of fragility of supercooled liquids with elastic properties of glasses. Phys Rev E 71:061501.
14. Ngai KL, Sokolov AP, Steffen W (1997) Correlations between boson peak strength and characteristics of local segmental relaxation in polymers. J Chem Phys 107:5268.

15. Tatsumisago M, Halfpap BL, Green JL, Lindsay SM, Angell CA (1990) Fragility of Ge-As-Se glass-forming liquids in relation to rigidity percolation, and the Kautzman paradox. Phys Rev Lett 64:1549–1552.

16. Ito K, Moynihan C, Angell CA (1999) Thermodynamic determination of fragility in liquids and a fragile-to-strong liquid transition in water. Nature 398:492–495.

17. Kamitakahara WA, Cappelletti RL, Boolchand P, Halfpap B, Gompf F, Neumann DA, Mutka H (1991) Vibrational densities of states and network rigidity in chalcogenide glasses. Phys Rev B 44:94–100.

18. Phillips JC (1979) Topology of covalent non-crystalline solids I: Short-range order in chalcogenide alloys. J Non-Cryst Solids 34:153–181.

19. Phillips JC, Thorpe MF (1985) Constraint theory, vector percolation and glass formation. Sol State Comm 53:699–702.

20. Böhmer R, Angell CA (1991) Correlations of the nonexponentiality and state dependence of mechanical relaxations with bond connectivity in Ge-As-Se supercooled liquids. Phys Rev B 45:10091–10094.

21. Micoulaut M, Boolchand P (2003) Comment on Microscopic Theory of Network Glasses. Phys Rev Lett 91:159601-1.

22. Wyart M, Nagel SR, Witten TA (2005) Geometric origin of excess low-frequency vibrational modes in weakly connected amorphous solids. Europhys Lett 72:486–492.

23. Wyart M (2005) On the rigidity of amorphous solids. Annales de Physique 30(3):1.

24. O'Hern CS, Silbert LE, Liu AJ, Nagel SR (2003) Jamming at zero temperature and zero applied stress: The epitome of disorder. Phys Rev E 68:011306.

25. Brito C, Dauchot O, Biroli G, Bouchand JP (2010) Elementary excitation modes in a granular glass above jamming. Soft Matter 6:3013–3022.

26. Xu N, Wyart M, Liu AJ, Nagel SR (2007) Excess vibrational modes and the Boson peak in model glasses. Phys Rev Lett 98:175502.

27. Brito C, Wyart M (2009) Geometric interpretation of previtrification in hard sphere liquids. J Chem Phys 131:024504.

28. Ghosh A, Chikkadi VK, Schall P, Kurchan J, Bonn D (2010) Density of states of colloidal glasses. Phys Rev Lett 105:248305.

29. Chen K, Ellenbroek WG, Zhang ZX, Chen DTN, Yunker PJ, Henkes S, Brito C, Dauchot O, van Saarloos W, Liu AJ, Yodh AG (2010) Low-frequency vibrations of soft colloidal glasses. Phys Rev Lett 105:025501.

30. Trachenko KO, Dove MT, Harris MJ, Heine V (2000) Dynamics of silica glass: two-level tunnelling states and low-energy floppy modes. J Phys: Cond Matt 12:8041–8064.

31. Liu AJ, Nagel SR, van Saarloos W, Wyart M (2010) in Dynamical Heterogeneities in Glasses, Colloids and Granular Media, eds Berthier L, Biroli G, Bouchaud JP, van Saarloos W (Oxford, New York).

32. Garboczi EJ, Thorpe MF (1985) Effective-medium theory of percolation on central-force elastic networks. II. Further results. Phys Rev B 31:7276–7681.

33. Boolchand P, Lucovsky G, Phillips JC, Thorpe MF (2005) Self-organization and the physics of glassy networks. Philos Mag 85:3823–3838.

34. Wyart M, Liang H, Kabla A, Mahadevan L (2008) Elasticity of floppy and stiff random networks. Phys Rev Lett 101:215501.

35. Düring G, Lerner E, Wyart M (2013) Phonon gap and localization lengths in floppy materials. Soft Matter 9:146–154.

36. Ellenbroek WG, Zeravcic Z, van Saarloos W, Hecke M (2009) Non-affine response: Jammed packings vs. spring networks. Europhys Lett 87:34004.

37. Wyart M (2010) Scaling of phononic transport with connectivity in amorphous solids. Europhys Lett 89(6):64001.

38. Grannan ER, Randeria M, Sethna PJ (1990) Low-temperature properties of a model glass. I. Elastic dipole model. Phys Rev E 41:7784.

39. Calladine CR (1978) Buckminster Fuller's tensegrity structures and Clerk Maxwell's rules for the construction of stiff frames. Int J Solids Struct 14:161–172.

40. Wyart M (2010) Correlations between Vibrational Entropy and Dynamics in Liquids. Phys Rev Lett 104:095901.

41. Hopfield JJ (1982) Neural networks and physical systems with emergent collective computational abilities. Proc Natl Acad Sci USA 79(8):2554-2558.

42. Hayes B (2002) The easiest hard problem. Am Sci 90(2):113–117.

43. Mertens S (2001) A physicist's approach to number partitioning. Theo Comp Sci 265:79–108.

44. Derrida B (1981) Random-energy model: An exactly solvable model of disordered systems. Phys Rev B 24:2613–2626.

45. Cherrier R, Dean DS, Lefèvre A (2003) Role of the interaction matrix in mean-field spin glass models. Phys Rev E 67:046112.

46. Caltagirone F, Ferrari U, Leuzzi L, Parisi G, Ricci-Tersenghi F, Rizzo T (2012) Critical slowing down exponents of mode coupling theory. Phys Rev Lett 108:085702.

47. Berthier L, Witten TA (2009) Compressing nearly hard sphere fluids increases glass fragility. Europhys Lett 86:10001.

48. Berthier L, Tarjus G (2011) Nonperturbative effect of attractive forces in viscous liquids. Phys Rev Lett 103:170601.

49. Cammarota C, Biroli G, Tarzia M, Tarjus G (2012) On the fragility of the mean-field scenario of structural glasses for finite-dimensional disordered spin models. arXiv:1210.2941.

50. Widmer-Cooper A, Pierry H, Harrowell P, Reichman D (2008) Irreversible reorganization in a supercooled liquid originates from localized soft modes. Nature Phys 4:711-715.

51. Lutsko JF (1989) Generalized expressions for the calculation of elastic constants by computer simulations. J Appl Phys 65:2991.

52. Karmakar S, Lerner E, Procaccia I. (2010) Athermal nonlinear elastic constants of amorphous solids. Physical Review E 82: 026105.

53. Ota R, Yamate T, Soga N, Kunugi M (1978) Elastic properties of Ge-Se glass under pressure. J Non-Cryst Solids 29:67–76.

54. Mahadevan S, Giridhar A, Singh AK (1983) Elastic properties of Ge-Sb-Se glasses. J Non-Cryst Solids 57:423–430.